

In vitro analysis of catalase and superoxide dismutase mimetic properties of blue tattoo ink

Homolak, Jan

Source / Izvornik: **Free Radical Research, 2022, 56, 343 - 357**

Journal article, Accepted version

Rad u časopisu, Završna verzija rukopisa prihvaćena za objavljivanje (postprint)

<https://doi.org/10.1080/10715762.2022.2102976>

Permanent link / Trajna poveznica: <https://urn.nsk.hr/urn:nbn:hr:105:168116>

Rights / Prava: [In copyright](#) / [Zaštićeno autorskim pravom.](#)

Download date / Datum preuzimanja: **2024-05-03**



Repository / Repozitorij:

[Dr Med - University of Zagreb School of Medicine
Digital Repository](#)



1 In vitro analysis of catalase and superoxide dismutase mimetic properties of blue tattoo ink

2
3 Jan Homolak^{1,2}

4 ¹ Department of Pharmacology, University of Zagreb School of Medicine, Zagreb, Croatia

5 ² Croatian Institute for Brain Research, University of Zagreb School of Medicine, Zagreb,
6 Croatia

7
8
9 Jan Homolak, MD

10 Department of Pharmacology,
11 University of Zagreb School of Medicine,
12 Salata 11, 10 000 Zagreb,
13 Croatia

14 homolakjan@gmail.com

15 00385 91 9411 468

Abstract

Tattoo inks are comprised of different combinations of bioactive chemicals with combined biological effects that are insufficiently explored. Tattoos have been associated with oxidative stress; however, a recent N-of-1 study suggested that blue tattoos may be associated with suppressed local skin oxidative stress. The present study aimed to explore the attributes of the blue tattoo ink (BTI) that may explain its possible effects on redox homeostasis, namely the catalase (CAT) and superoxide dismutase (SOD)-mimetic properties that have been reported for copper(II) phthalocyanine (CuPC) – the main BTI constituent. Intenze™ Persian blue (PB) BTI has been used in the experiment. CAT and SOD-mimetic properties of PB and its pigment-enriched fractions were analyzed using the carbonato-cobaltate (III) formation-derived H₂O₂ dissociation and 1,2,3-trihydroxybenzene autooxidation rate assays utilizing simple buffers and biochemical matrix of normal skin tissue as chemical reaction environments. CuPC-based tattoo ink PB and both its blue and white pigment-enriched fractions demonstrate CAT and SOD-mimetic properties *in vitro* with effect sizes demonstrating a substantial dependence on the biochemical environment. PB constituents act as inhibitors of CAT but potentiate its activity in the biochemical matrix of the skin. CuPC-based BTI can mimic antioxidant enzymes, however chemical constituents other than CuPC (e.g. the photoreactive TiO₂) seem to be at least partially responsible for the BTI redox-modulating properties.

Keywords: tattoo; tattoo ink; oxidative stress; catalase; superoxide dismutase

Conflict of interest statement: No conflict of interest to disclose.

Funding source: None.

Introduction:

The art of tattooing dates back to the earliest stages of tribal communities and the oldest known tattoo belongs to the famous mummy *Ötzi the Iceman* (3000 BC)[1]. Throughout history, the prevalence of tattoos varied; however, in the last decades, the practice of tattooing spread throughout the Western world and became a mainstream form of body art. Recent estimates suggest that up to 25% of Europeans under the age of 20 and up to 38% of Americans under the age of 29 bear at least one tattoo [2]. Despite the omnipresence of tattooing, the biomedical effects of tattoos remain poorly explored, possibly because tattoo inks are comprised of different combinations of many bioactive chemicals with combined biological effects that are challenging to explore, let alone predict. In general, tattoo inks contain: i) organic (e.g. azo or polycyclic aromatic) or inorganic pigments (e.g. titanium dioxide (TiO₂), barium sulfate (BaSO₄), iron oxide, chromium oxide); ii) binders (e.g. polyethylene glycol, polyvinylpyrrolidone); iii) solvents (e.g. water, alcohol); and iv) additives (preservatives, surfactants)[2]. Additionally, impurities (e.g. nitrosamines or formaldehyde) may be present as well, and the ink injected into the body may contain nickel and chromium particles shredded from the needle during tattooing [3]. During the procedure of tattooing, all the constituents are delivered into the dermis where they become 100% systemically bioavailable due to direct contact with the blood and lymph. Although the kinetics of different tattoo ink constituents is still unknown, it is assumed that soluble components undergo rapid systemic distribution, while the insoluble pigments are mostly retained in the area of injection and in the draining lymph nodes where they may exert biological effects [2].

Although substantial efforts have been made to better understand the biological effects of tattoo inks utilizing *in vitro* and *in vivo* models, the results demonstrate that the observed effects are strongly dependent on the chemical constitution of the ink and the toxicological model utilized in the study. For example, Falconi et al. reported reduced viability and expression of the procollagen $\alpha 1$ type I in primary human fibroblasts incubated with *Biolip 27* but not *Strong black* [4]. Regensburger et al. reported substantial variability in the potency of 19 commercially available tattoo inks in respect to their inhibitory effects on mitochondrial activity in primary human dermal keratinocytes exposed to UVA radiation [5]. Arl et al. compared the effects of blue, green, red, and black tattoo ink on cell viability and the generation of reactive oxygen species (ROS) and reported that incubation with red and green tattoo inks induced the most pronounced toxic effects on the human keratinocyte cell line [6]. Perplexing *in vivo* results have also been reported. For example, in studies on tattoo ink carcinogenicity, it has been reported that mice tattooed with red tattoo ink and exposed to ultraviolet radiation develop tumors slightly faster (214 vs 224 days) and show an increased tumor growth rate in comparison with sham-tattooed mice [7]. In contrast, black tattoo ink was protective against ultraviolet radiation-induced squamous cell carcinoma, delaying the tumor onset by approximately 50 days in tattooed mice [8]. Although it will be interesting to see the follow-up studies on the interaction between exposure to different tattoo inks and the carcinogenic potential of ultraviolet radiation (to address the uncertainty related to relatively small effects reported in [7] and [8]), the apparently discrepant results provide a good illustration of the fact that the biological effects of different tattoo inks seem to be too complex and specific to provide foundations for inductive reasoning on the effects of tattoo inks in general. To better understand the biomedical consequences of tattooing, a substantial effort should be made to i) elucidate the biological effects of individual chemicals present in different tattoo inks, and ii) explore

the synergistic, additive, or antagonistic effects of chemical constituents of different tattoo inks in model systems that resemble those found *in vivo*.

The present aim was to explore the properties of blue tattoo ink that may explain the recently reported observation that a blue tattoo was able to suppress local skin oxidative stress [9]. Oxidative stress is a pathophysiological condition that ensues as a consequence of the inability of a system to maintain the balance between the electrophilic and the nucleophilic arm of redox homeostasis [10]. Considering redox homeostasis is critical for normal cellular functioning, it is no surprise that oxidative stress has been recognized as an important etiopathogenetic factor and a promising pharmacological target in pathophysiological conditions of the skin [11,12]. Tattoo inks have generally been associated with increased levels of oxidative stress (e.g. [5,6,13–15]); however, this has so far only been supported by indirect findings from *in vitro* experiments and there is currently no direct evidence for tattoo-induced oxidative stress in humans. In contrast, there is some evidence indicating that blue tattoo ink may be able to reduce oxidative stress. In an N-of-1 study, skin tattooed with blue tattoo ink demonstrated increased surface reductive capacity and the interstitial and intracellular fluid-enriched capillary blood from the tattoo had an increased content of protein sulfhydryls, reductive capacity, and catalase (CAT) activity, and reduced lipid peroxidation in comparison with the sample obtained from nontattooed skin [9]. Copper(II) phthalocyanine (CuPC), the main constituent of blue tattoo inks, can both reduce and prevent lipid peroxidation in homogenates of the mouse brain, kidney, and liver and exerts a substantial protective effect in the deoxyribose degradation assay [16]. Furthermore, it has been reported that CuPC can act as a dual functional mimetic of CAT and superoxide dismutase (SOD), two important antioxidant enzymes and that this property may be responsible for its lipid peroxidation-suppressing effects [17].

The present study aimed to explore whether: i) a blue CuPC-based tattoo ink can act as a CAT and SOD mimetic *in vitro*; ii) CAT and SOD mimetic properties of blue tattoo ink are primarily present in the CuPC-enriched ink fraction; iii) blue tattoo ink and its CuPC-enriched and residual fractions potentiate or inhibit the effects of CAT and SOD in the complex biochemical matrix of normal skin tissue (i.e. in the presence of endogenous CAT, SOD, and regulators of their activity); iv) components of the tattoo ink may directly interact with components of the skin.

Materials and methods:

Sample preparation

Intenze™ Persian blue tattoo ink (PB) (Intenze, USA) was used in the experiment. The ingredients declared on the official material safety data sheet included: H₂O (The European Community number (EC): 231-791-2), BaSO₄ (EC: 231-784-4), TiO₂ (EC: 215-280-1), CuPC (EC: 205-685-1), glycerine (EC: 200-289-5), isopropyl alcohol (EC: 200-661-7), *Hamamelis Virginiana* L. extract (EC: 283-637-9). Diluted PB samples were obtained by v/v dilution in pre-defined ratios in double-distilled H₂O (ddH₂O; 0.055 µS/cm). Dye fractionation was done by differential centrifugation. PB was first spun down for 30 minutes at a relative centrifugal force (RCF) of 12879 x g, and then the same process was repeated twice with both the supernatant (blue fraction) and the pellet (white fraction). The supernatant of the blue pigment-enriched fraction and the pellet of the white pigment-enriched fraction were used for subsequent analyses.

UV-Vis spectrophotometry

UV-Vis spectra were obtained by scanning the absorbance in the wavelength range from 220 nm to 750 nm using The NanoDrop® ND-1000 (Thermo Fisher Scientific, USA).

Catalase-like activity

CAT solution was prepared by dissolving 1 mg of lyophilized bovine liver CAT powder (Sigma Aldrich, USA) in 10 ml of phosphate-buffered saline (PBS) (pH 7.4). CAT activity was measured using the method first described by Hadwan [18] and adapted in [19]. Briefly, the samples were incubated with 50 µl of the substrate solution (2-10 mM H₂O₂ in PBS) and the reaction was stopped by adding 150 µl of the Co(NO₃)₂ stop solution (5 mL Co(NO₃)₂ x 6 H₂O (0.2 g in 10 mL ddH₂O) + 5 mL (NaPO₃)₆ (0.1 g in 10 mL ddH₂O) added to 90 mL of NaHCO₃ (9 g in 100 mL ddH₂O)). The concentration of H₂O₂ was determined indirectly by measuring the absorbance of the carbonato-cobaltate (III) complex ([Co(CO₃)₃]Co) at 450 nm using the Infinite F200 PRO multimodal microplate reader (Tecan, Switzerland). Due to interference, a unique baseline model was established for each sample by simultaneous incubation with substrate solutions of graded nominal concentrations between 1 and 10 mM H₂O₂ and the Co(NO₃)₂ stop solution. The amount of residual H₂O₂ was estimated from the model for each sample and each time-point. CAT activity was assessed indirectly based on permutation-derived estimates of the baseline values (t = 0 s) and final values (t₁ = 60 s or 300 s)[20].

Superoxide dismutase-like activity

The SOD-like activity was measured by assessing the inhibition of 1,2,3-trihydroxybenzene (THB) autoxidation rate [21,22]. Briefly, 5 µl of each sample was placed in a 96 well-plate and incubated with freshly pre-mixed THB working solution (64 µl of 60 mM THB dissolved in 1 mM HCl mixed with 3400 µl of 0.05 M Tris-HCl and 1 mM Na₂EDTA adjusted to pH 8.2). THB autoxidation was measured by assessing the absorbance increment at 450 nm with repeated measurements obtained by the Infinite F200 PRO multimodal microplate reader (Tecan, Switzerland).

Preparation of the skin tissue constituents as the reaction matrix

To test whether the effects observed *in vitro* would be affected by the presence of skin tissue constituents present *in vivo*, a rat skin homogenate was prepared. Briefly, a piece of skin from a single rat euthanized in deep anesthesia (70 mg/kg ketamine; 7 mg/kg xylazine) was dissected and stored at -80 °C. The animal was in the control (untreated) group of another experiment and the tissue was dissected after decapitation in concordance with the 3Rs concept [23] in order not to interfere with the experimental protocol. The animal study from which the tissue was obtained was approved by the Ethics Committee of The University of Zagreb School of Medicine (380-59-10106-18-111/173) and the Croatian Ministry of Agriculture (EP 186/2018). The skin was rapidly dissected from the surrounding adnexa and placed in 1000 µl of lysis buffer (150 mM NaCl, 50 mM Tris-HCl, 1 mM EDTA, 1% Triton X-100, 1% sodium deoxycholate, 0.1% SDS, 1 mM PMSF, protease inhibitor cocktail (Sigma-Aldrich, USA) and PhosSTOP phosphatase inhibitor (Roche, Switzerland) adjusted to pH 7.5) on ice. The tissue was homogenized using Microson Ultrasonic Cell Disruptor (Misonix, SAD), centrifuged for 10 min at 4 °C, and RCF of 12 879 × g, and the supernatant was stored at -80 °C. For the acute experiments, 5 µl of the tissue homogenate was used per well, and for the pretreatment experiments, 45 µl of the skin homogenate was incubated with either 5 µl of dd H₂O, or 5 µl of the sample (1:10 PB, 1:10 blue, and 1:10 white fraction) for 180 min at 37°C. Bradford's

analysis of the protein concentration (using the bovine serum albumin (BSA) standard) indicated the biochemical matrix of the skin contained 4.37 µg protein per µl.

Lateral flow assay for the assessment of the interaction between the constituents of the tattoo ink and components of the skin, albumin, and catalase

A lateral flow assay (LFA) was conducted to assess the interaction between chemical constituents of the blue tattoo ink and biochemical components of the skin. Additionally, the LFA was employed to test the interaction of tattoo ink with catalase (to address the possibility of direct interaction as a mediator of biological effects), and BSA as a standard protein with a large intrinsic binding potential for a large diversity of small molecules. All samples (skin homogenate, CAT, BSA) were spotted onto the nitrocellulose strips (0.45 µm pore size; Amersham Protran; GE Healthcare Life Sciences, USA) in a way that each strip contained the free route for the uninterrupted analyte flow (control lane) and the sample-capturing lane (experimental lane). The membranes were left to air-dry for 15 minutes. Once dry, the strips were fixed in the glass holder in a way that the proximal end was available for the administration of the analyte (tattoo ink) followed by administration of the same volume of vehicle (ddH₂O) to remove excess PB. An additional LFA experiment was conducted using nitrocellulose spotted PB and its blue and white fractions as the stationary samples and ddH₂O as the mobile phase. In both experiments, analyte mobility was recorded and the signal density line profiles of the control and experimental lane for each sample were subsequently extracted for 5 time-points using Fiji (NIH, USA).

Tattoo ink interaction electrophoretic mobility shift assays

Electrophoretic mobility shift assays (EMSA) were conducted to complement the LFA and provide additional information on the nature of the interaction between skin components and the tattoo ink constituents. Sample pre-incubation EMSA (SP-EMSA) was done by analyzing the mobility interference using parallel electrophoretic separation of the tattoo ink-treated and “naïve” skin homogenates and CAT. Pre-treated samples were incubated with PB to achieve a 1:100 dilution of the ink, while the control samples were incubated with an equal volume of vehicle (ddH₂O). The samples were mixed with the modified bromophenol blue-free sample buffer 4x stock containing 40% glycerol, 8% SDS, 200 mM Tris HCl (so that bromophenol blue does not interfere with the CuPC color), incubated with the sample buffer for 10 minutes at 95°C, and loaded onto the TGX Stain-Free FastCast 12% polyacrylamide gels (Bio-Rad, USA) for electrophoretic separation. Spectral analysis of gels was done by ChemiDoc MP Imaging System (Bio-Rad, USA). Transfer onto the nitrocellulose was done using the Trans-Blot Turbo semi-dry transfer system (Bio-Rad, USA). The elution of CAT from the nitrocellulose (for subsequent spectral analysis) was done by incubating cut-out proteins in the 50% pyridine in 0.1 M ammonium acetate (v/v; pH 8.9) for 120 min at 37 °C [24]. In addition to SP-EMSA, the interaction of the electrophoretically immobile CuPC with skin constituents and CAT was studied using the CuPC-capturing gradient electrophoretic separation (CCG-EMSA). Briefly, a capturing gel containing gradient concentrations of 1:850 PB mixed with a standard stacking polyacrylamide matrix was placed on top of the separating gel, and the skin and CAT samples were subjected to the electrophoretic separation to analyze the interaction of increased electrophoretic CuPC exposure (increased CuPC matrix path) and sample mobility.

Data analysis

Data were analyzed in R (4.1.0). In the experiments where multiple substrate concentrations and multiple substrate exposure times were used, CAT-like activity was analyzed using linear regression with enzymatic activity (permutation-derived estimates) defined as the dependent variable and sample, substrate concentration, and time defined as independent variables. Model assumptions were checked by visual inspection of the residual and fitted value plots. Model outputs were reported as point estimates of least-square means with accompanying 95% confidence intervals. Comparisons of the samples from the model were reported as effect sizes (differences of estimated marginal means with accompanying 95% confidence intervals). Alpha was set at 5% and p-values were adjusted using the Tukey method.

Results:

Persian blue tattoo ink acts as a weak catalase and superoxide dismutase mimetic *in vitro*

PB demonstrated dilution-dependent CAT-like activity *in vitro*, with the 1:10 dilution showing the ability to dissociate ~0.9 mM of H₂O₂ in 300 s on average, in substrate concentrations ranging from 6 to 10 mM (**Fig 1A**). PB (1:10) dissociated 0.6 mM of H₂O₂ in the presence of 10 mM H₂O₂ and 1 mM when incubated with 8 and 6 mM, indicating lower efficacy at high substrate concentrations. The 1:100 dilution of PB demonstrated no CAT-like activity. The largest tested PB concentration (1:10) exerted SOD-like activity as well, by reducing the rate of THB autoxidation in the first 300 s of the assay. After 300 s, the maximum suppressive capacity of 1:10 PB was reached and PB potentiated autoxidation (**Fig 1B**). Lower PB concentrations (1:100; 1:1000; 1:10 000) showed no SOD-like activity.

Blue and white fractions of the Persian blue tattoo ink show no catalase mimetic properties, but demonstrate divergent superoxide dismutase-like behavior

Centrifugation-based fractionation of PB yielded a blue CuPC-enriched fraction and a white fraction most likely enriched with TiO₂ and BaSO₄ (**Fig 2A**). UV-Vis spectra of fractionated samples suggested that CuPC was primarily present in the blue fraction, as evident by the presence of the Soret peak (B-band) and the Q-band with the Davydov splitting characteristic for the phthalocyanine derivatives [25,26] (**Fig 2B**). Neither the blue nor the white fraction demonstrated CAT-like activity *in vitro* (**Fig 2C-E**). Interestingly, „negative estimates of the activity“ were obtained for the 1:10 dilution of both fractions indicating possible photocatalytic generation of H₂O₂ [27]. The observed effect was substrate concentration-dependent and more pronounced for the white fraction, which also demonstrated a pronounced time-dependence (**Fig 2C-E**). While the CuPC-enriched blue fraction showed no SOD-like activity at $t < 300$ s, the white fraction (1:10) potentiated THB autoxidation. At $t > 300$ s, the blue PB fraction (1:10) demonstrated SOD-like activity (**Fig 2F**).

Persian blue tattoo ink and its blue and white pigment-enriched fractions inhibit catalase *in vitro* but potentiate its action in the presence of biochemical constituents of the skin

Apart from acting as CAT/SOD mimetics, PB constituents may modulate redox balance by affecting the activity of endogenous enzymes. In the presence of bovine liver CAT, the CuPC-enriched PB fraction acted as a weak CAT inhibitor with no evident dose-response, while PB and the white fraction exhibited a pronounced dose-dependent inhibition of the enzyme (**Fig 3A, B**). A different pattern was observed in the presence of biochemical constituents of the skin, where PB and its blue and white pigment-enriched fractions acted as potentiators of

endogenous CAT, with the largest effect observed in the presence of the white fraction (**Fig 3C, D**). As the acute effects may not faithfully represent biochemical effects that may take place *in vivo*, an additional experiment was conducted in which the tested samples were first incubated with the biochemical constituents of the skin. Interestingly, following prolonged incubation (180 min at 37 °C), the pronounced effect of the white fraction was substantially attenuated, and the CuPC-enriched fraction induced the most pronounced effect on the activity of endogenous CAT (**Fig 3E, F**). In the presence of tissue constituents, both the blue and white fractions acted as SOD mimetics at $t < 300$ s, while there was no difference between the effect of PB and the control condition (**Fig 3G**). After the 300 s time-point, the CuPC-enriched fraction demonstrated stable SOD mimetic activity, while the white fraction potentiated THB autoxidation (**Fig 3G**). Following the prolonged incubation at 37 °C, SOD potentiating effects of PB and its blue and white fractions were completely lost (**Fig 3H**).

Constituents of the blue tattoo ink interact with components of the biochemical matrix of the skin

To better understand the nature of the observed effects chemical interaction between constituents of the tattoo ink and the components of the biochemical matrix of the skin was evaluated using the LFA, SP-EMSA, and CCG-EMSA. LFA indicated that skin homogenate, CAT, and BSA can all interact with constituents of PB that exhibit nitrocellulose lateral flow (Fig 4A). BSA demonstrated the largest PB flow-disrupting capacity both in terms of binding the flow front and resistance to subsequent elution by vehicle. Both CAT and the biochemical matrix of the skin were also able to bind the PB front and resist ddH₂O elution (Fig 4A). Interestingly, upon elution, the skin homogenate demonstrated a wave pattern suggesting the presence of interaction with several separate components (Fig 4B). The CCG-EMSA and SP-EMSA were used as complementary methods to better understand the nature of the observed interaction. The CCG-EMSA revealed that the observed CAT-binding properties of PB were not able to resist the electrophoretic mobility of the enzyme indicating that the nature of the interaction was i) too weak to affect the electrophoretic flow, or ii) incompatible with the unfolded linear structure and/or negative charge introduced by the reductive environment and SDS (Fig 4C). Interestingly, although there was no evident electrophoretic mobility shift introduced by increasing path length through the PB-enriched stacking polyacrylamide for CAT this was not the case with skin homogenate where CCG-EMSA revealed a pronounced dose-response electrophoretic mobility shift regardless of the reducing environment and high SDS concentration (Fig 4C). The SP-EMSA confirmed the aforementioned findings as CAT electrophoretic mobility was relatively resistant to the effects of PB, while tattoo ink decelerated mobility of some biochemical constituents of the skin – speaking in favor of binding even in the reductive environment and in the presence of high SDS (Fig 4D). The exact chemical component (or components) of the ink responsible for the electrophoretic mobility shift, as well as primary components of the skin responsible for the observed interaction, remain to be further explored. Nevertheless, spectral analysis of the electrophoretic and lateral flow mobility membranes/gels provided additional information that may lay the groundwork for a better understanding of the observed interaction in the future. The SP-EMSA experiments suggest that the blue pigment (CuPC) demonstrates electrophoretic mobility only in the stacking polyacrylamide matrix (Fig 5A). Such a pattern indicates that CuPC either i) moves on its own in the electrical field achieved in the polyacrylamide gel electrophoresis (PAGE) setup (i.e. exerts electrophoretic mobility), or ii) moves together with CAT and some components of the skin as a result of molecular interactions that cannot withstand the resistance

of mobility through the dense portion of the resolving polyacrylamide. Electrophoretic mobility experiments with PB gradient stacking gel support latter as penetrance of the blue pigment didn't increase (or possibly even decreased) as a result of increased vertical exposure (Fig 5B) suggesting that the mobility shift of the skin homogenates may have been the result of the interactions at the level of capturing-adapted stacking polyacrylamide. Nevertheless, it is possible that i) some CuPC remained bound to proteins and caused electrophoretic deceleration in quantities that are too small to be detected by simple visual inspection, and/or ii) some other constituents of the tattoo ink demonstrated protein binding and caused deceleration in the resolving fraction of the gel. To test this, spectral analysis of LFA membranes and electrophoretic mobility gels was conducted. Spectral analysis of the LFA membranes revealed that the LFA mobility pattern of PB and both its blue and white fractions demonstrate at least 3 general patterns: the sample pool (the area where the sample was deposited); the middle mobile phase (largely absent in the white fraction); and the mobile front (present in all samples)(Fig 5C). The sample pool and the middle mobile phase demonstrated a satisfactory quantum yield upon excitation (EX) at 302 nm combined with the wide 535-645 nm emission (EM) filter. All 3 LFA patterns (the sample pool and both mobile phases) for PB, blue, and white fractions were successfully visualized under 755-777 nm EX with the 810-860 nm EM filter, and a variety of conditions (e.g. EX/EM(nm): 460-490/518-546; 520-545/577-613; 625-650/675-725; 650-675/700-730) were found to enable a good representation of the mobile front (Fig 5C). Spectral analysis of the LFA membranes from the experiment with spotted CAT and biochemical matrix of the skin revealed that, in addition to the interaction with the blue fraction of the ink, both samples also captured components of the ink most likely representing the mobile front from the LFA experiment in which PB was used as the mobile phase (with CAT sample demonstrating greater mobile front binding capacity than the skin sample)(Fig 5D). Although treatment-naïve CAT has been shown to emit in the close spectral range (control CAT; Fig 5D), the comet pattern indicates the observed signal was most likely from the component of the mobile phase and not an endogenous signal from the spotted sample. Spectral analysis of the SP-EMSA polyacrylamide gels provides further evidence supporting the hypothesis that, in addition to CuPC, other components of the tattoo ink (primarily present in the white fraction) may interact with CAT and constituents of the skin (and affect their electrophoretic mobility)(Fig 5E). Spectral analysis of the SP-EMSA polyacrylamide gels confirms the observations from the LFA and indicates that another PB component (most likely originating from the white fraction) enters the resolving polyacrylamide (alone or bound to sample constituents) and possibly affects the sample electrophoretic mobility (even after accounting for the baseline spectral properties of PB and its blue and white fractions and the effects of the tattoo ink concentration)(Fig 5E, F). Interestingly, the presence of the component of the white fraction seems to have functional consequences as the ink-exposed sample shows the ability to potentiate the chemiluminescent reaction of luminol and H₂O₂ (Fig 5G). To ensure that the observed effect was not due to the presence of CuPC present in quantities that are too small to be detected by visual inspection, both CAT samples were eluted from the membrane and subjected to spectral analysis (Fig 5H). To further ensure no CuPC was present, UV-Vis spectra of the eluates were measured and compared to the spectra of the same samples before PAGE showing a clear disappearance of the Q-band with the Davydov splitting characteristic for the phthalocyanine derivatives (Fig 5I).

Discussion:

The presented results support the hypothesis that PB, a blue CuPC-based tattoo ink, can act as a mimetic of CAT and SOD and provide a possible mechanistic explanation for the reduced levels of oxidative stress in the skin with a blue tattoo [9]. Although CuPC can act as a dual functional mimetic of CAT and SOD and suppress lipid peroxidation *in vitro* [17], it was hypothesized that the *a priori* assumption that PB would necessarily reflect the properties of its main component (CuPC) would be unjustified considering the unspecified concentration of CuPC and the presence of other chemicals that may theoretically annihilate or even reverse its potential antioxidant effects. The results indicate the caution was reasonable. Although PB demonstrated CAT and SOD-like activity, the observed H₂O₂ dissociation capacity was relatively modest, and SOD-like activity was present only in the first part of the assay and demonstrated high variability across trials (**Fig 1**). Furthermore, the CAT-mimetic action was not persuasive once PB was fractionated (**Fig 2C-E**), while the SOD-like activity of the fractions (**Fig 2F**) suggested that the large variability and time-dependence observed in the first experiment (**Fig 1B**) may have reflected the opposing effects of chemical constituents on THB autoxidation. Despite the initial hypothesis that CuPC may be the main chemical constituent of tattoo ink responsible for the effects of a blue tattoo on skin redox homeostasis [9], potentiation of THB autoxidation by the white PB fraction (**Fig 2F**) indicated that there are likely at least two chemical mediators with possibly opposing actions. Although it was not possible to confirm the presence of individual chemical constituents in PB fractions, it is highly likely that BaSO₄ and TiO₂ were the main constituents of the white fraction, and that they may be responsible for the observed potentiation of THB autoxidation. Although both BaSO₄ and TiO₂ can induce oxidative stress in different models [28,29], TiO₂ may be a more likely mediator of the observed effect, as it stimulates the expression of antioxidant defense systems to a greater extent *in vitro* [30]. In addition, TiO₂ can generate superoxide radicals and other ROS by reducing oxygen, due to an increased number of conduction band electrons following light exposure [27,31]. In the context of the effects of blue and white PB fractions on SOD activity, the reported time-dependence of SOD-mimetic properties of PB (**Fig 1B**) may be related to the limited ability of blue fraction constituents to suppress THB autoxidation, potentiated by the chemicals present in the white fraction of the ink.

In addition to the observed CAT/SOD-mimetic activity *in vitro*, in order to affect redox balance *in vivo*, tattoo ink should be able to exert the effect in the presence of the complex biochemical matrix of normal skin tissue (i.e in the presence of endogenous CAT, SOD, and regulators of their activity). In the presence of CAT, PB inhibited the H₂O₂ dissociation rate with the most pronounced inhibition observed with the white ink fraction (**Fig 3A, B**). Although little is known about the effects of BaSO₄ on CAT activity, it has been shown that TiO₂ can bind to CAT via electrostatic and hydrogen bonding forces, destabilize its structure and affect its activity in a dose-dependent manner [32]. Interestingly, the effects of tattoo ink on CAT were drastically altered in the presence of the biochemical constituents of normal skin, as all tested samples potentiated the relatively low endogenous H₂O₂ dissociation potential (**Fig 3C, D**). The white fraction of the ink induced the most pronounced effect, increasing the activity 78-fold, while the blue fraction induced only „a modest” ~5-fold increment. A substantial increment in the dissociation potential observed with the white fraction is in line with the SP-EMSA results indicating that a constituent of the ink that does not contain CuPC (most likely originating from the white fraction) has a pronounced ability to degrade H₂O₂ (**Fig 5G-I**). Interestingly, the potentiation of CAT observed with the unfractionated ink was somewhere in

between (~17-fold), indicating that chemical constituents of tattoo ink might either act as competitive activators or engage in some other form of interaction that is reflected in CAT activity. A similar pattern was observed regarding the SOD-mimetic action, where the constituents from the blue and white fractions exhibited SOD-like properties on their own but canceled each other out when added to the tissue homogenate together (PB) (**Fig 3G**). Why were both ink fractions able to potentiate SOD activity, and whether the observed effect was mediated by the intrinsic SOD-mimetic properties of the chemical constituents or their action on the endogenous enzyme, defies a simple explanation and remains to be further explored. Nevertheless, considering that TiO₂ can potentiate the activity of SOD [33], one possibility is that TiO₂ may exert a dose-dependent modulatory effect on SOD similarly as has been shown for CAT [32].

Finally, the effects of PB and its fractions have been tested upon prolonged (180 min) incubation with skin homogenates at homeothermic temperature (37 °C), to assess whether some of the effects may be transient (e.g. due to dependence on an endogenous substrate) and affected by physiological temperature. Interestingly, both CAT and SOD-mimetic properties were dramatically altered by pre-incubation and the most pronounced H₂O₂ dissociation rate was observed for the blue ink fraction followed by PB (**Fig 3E, F**). The SOD-mimicking effect was annihilated by the pre-incubation procedure (**Fig 3H**). The exact nature of the observed phenomenon and whether the homeothermic pre-incubation more faithfully reflects the fate of the tattoo ink constituents in the human skin remains to be elucidated. On one hand, prolonged incubation at physiological temperature may provide more accurate environmental conditions for the biochemical reactions that may take place in the human body. On the other hand, the observed potentiation of the enzymatic activity may be dependent on a particular substrate present in the biochemical matrix of the tissue homogenate in limited quantities (in contrast to its continuous influx *in vivo*). Another possible explanation for the observed discrepancy might be a temperature-induced change in physicochemical properties of the tattoo ink constituents. Tattoo inks contain nanoparticles and both CuPC and TiO₂ can be found in the nanoparticle form in the blue tattoo ink (with the mean diameter of the CuPC/TiO₂ being 167 nm for the Intenze™ blue tattoo ink)[34,35]. Nanoparticles have an intrinsic potential to generate ROS, which has been recognized as a key mediator of nanotoxicity [36]. Considering that toxicity, photoreactivity, and ROS-generating potential depend on the particle size, shape, surface characteristics, and the crystal structure [31], a hypothetical reaction between the tattoo ink and either the tissue homogenate or the microtiter plate that may alter the structure of its nanoparticle components may provide an explanation for the observed alteration of the modulatory activity on CAT and SOD (**Fig 3**).

To further elucidate the nature of the CAT and SOD-mimetic actions of the blue tattoo ink a series of experiments was done to explore whether the observed functional alterations are accompanied by the ability of ink constituents to bind to CAT and the components of the skin matrix (Fig 4,5). Specific studies focused on the interaction of individual components are yet to be done. Nevertheless, preliminary experiments assessing a more general overview of the possibility that two complex and heterogeneous samples (tattoo ink and skin) contain molecules that show the ability to interact directly presented here (Fig 4,5) support the notion that the observed changes in the enzymatic activity may be a consequence of the interaction of at least several separate molecular entities from the skin, and definitely more than one chemical constituent of the tattoo ink.

In the context of previously reported redox-related changes in the skin with a blue tattoo, the results presented here support the hypothesis that the suppression of oxidative stress in the N-of-1 study may be related to the antioxidant properties of some constituents present in blue tattoo ink [9]. In the N-of-1 study, a 15% reduction in lipid peroxidation in the blue tattoo was associated with 11.8% greater CAT activity [9]. In concordance with this, in this study, the constituents of blue tattoo ink were able to potentiate CAT activity in the presence of the biochemical components of the skin (**Fig 3C-F**). Interestingly, in the same study, SOD activity was slightly higher in the tattoo sample; however, this result was taken as highly uncertain considering the difference was in the range of the coefficient of variation of the method [9]. In the context of the *in vitro* results presented here, it can be assumed that apart from the limited precision of the utilized method, SOD activity in the blue tattoo may have been unchanged due to the opposing action of different constituents of the tattoo ink (**Fig 3G**) or due to the same phenomenon responsible for the loss of SOD-mimetic activity following prolonged incubation at 37°C (**Fig 3H**).

Conclusion:

The presented results confirm the hypothesis that blue, CuPC-based tattoo ink can act as a CAT and SOD mimetic *in vitro* and provide evidence that the antioxidant effects of a blue tattoo *in vivo* [9] may be mediated by the ability of CuPC and other chemical constituents of the blue tattoo ink to mimic the activity of endogenous antioxidant enzymes. In contrast to the assumption that the CAT and SOD-mimetic properties of the tattoo ink would be primarily explained by the presence of CuPC, the results suggest that both the CuPC-enriched blue and the residual white fraction may exert CAT and SOD-mimetic properties and affect redox balance, indicating that other chemical constituents (e.g. TiO₂) may also be involved in modulation of redox homeostasis. Finally, it has been demonstrated that the ability of different constituents of the tattoo ink to potentiate and/or inhibit the activity of CAT and SOD depends on numerous factors (e.g. the presence of other constituents that exert synergistic, additive, or antagonistic effects; the concentration of the constituents and/or the substrate; the presence of compounds from the biochemical matrix of the skin; the incubation time and temperature) that should be taken in account.

Limitations:

Several important limitations should be emphasized. First, it was not possible to analyze the presence, or the quantity of individual chemical constituents of the tattoo ink used in the experiment, and the presence of different chemicals was assumed based on the official material safety data sheet of the product. Apart from the CuPC that was most likely present based on the UV-Vis spectrum characterized by the Soret peak (B-band) and the Q-band with the Davydov splitting characteristic for the phthalocyanine derivatives, the existence of other chemicals (and possibly also impurities) could not have been confirmed experimentally. Furthermore, the presence of CuPC and TiO₂ nanoparticles was assumed based on the experimental data for the Intenze™ blue tattoo ink reported by Høgsberg et al. [35], however, the existence or the size of nanoparticles was not confirmed experimentally and the potential influence of the experimental conditions on the particle aggregation, size, shape, surface characteristics, or the crystal structure (important for the redox-related effects) was not assessed. Finally, the possibility that the chemical reaction with some of the reagents may have introduced bias in some measurements can never be completely ruled out. For example, it has been observed that 450 nm absorbance of some of the dilutions of some fractions was affected

by spectrophotometric measurements (possibly due to light exposure as some chemical constituents such as TiO₂ act as well-known photocatalysts [27])(**Supplement**). Nevertheless, precautionary steps were taken to prevent the chemical bias that may have been introduced due to unforeseen chemical reactions of samples and reagents (e.g. baseline validation model was established and analyzed for each sample individually to ensure that the expected changes such as the dissociation of H₂O₂ can be assumed and quantified without the risk of chemical interaction) (**Supplement**).

Funding source:

None.

Conflict of interest statement:

No conflict of interest to disclose.

Data availability statement:

Data can be obtained from the author's GitHub repository (<https://github.com/janhomolak>).

Author's contributions:

JH conceived the study, conducted the experiments, analyzed data, and wrote the manuscript.

References:

- [1] Pesapane F, Nazzaro G, Gianotti R, et al. A short history of tattoo. *JAMA Dermatol* 2014;150:145.
- [2] Giubudagian M, Schreiber I, Singh AV, et al. Safety of tattoos and permanent make-up: a regulatory view. *Arch Toxicol* 2020;94:357–369.
- [3] Schreiber I, Hesse B, Seim C, et al. Distribution of nickel and chromium containing particles from tattoo needle wear in humans and its possible impact on allergic reactions. *Particle and Fibre Toxicology* 2019;16:33.
- [4] Falconi M, Teti G, Zago M, et al. Influence of a commercial tattoo ink on protein production in human fibroblasts. *Arch Dermatol Res* 2009;301:539–547.
- [5] Regensburger J, Lehner K, Maisch T, et al. Tattoo inks contain polycyclic aromatic hydrocarbons that additionally generate deleterious singlet oxygen. *Exp Dermatol* 2010;19:e275-281.
- [6] Arl M, Nogueira DJ, Schweitzer Köerich J, et al. Tattoo inks: Characterization and in vivo and in vitro toxicological evaluation. *J Hazard Mater* 2019;364:548–561.
- [7] Lerche CM, Heerfordt IM, Serup J, et al. Red tattoos, ultraviolet radiation and skin cancer in mice. *Experimental Dermatology* 2017;26:1091–1096.
- [8] Lerche CM, Sepehri M, Serup J, et al. Black tattoos protect against UVR-induced skin cancer in mice. *Photodermatol Photoimmunol Photomed* 2015;31:261–268.
- [9] Homolak J. The effect of a color tattoo on the local skin redox regulatory network: an N-of-1 study. *Free Radic Res* 2021;1–9.
- [10] Homolak J. Redox Homeostasis in Alzheimer's Disease. *Redox Signaling and Biomarkers in Ageing* 2021;

- 523 [11] Rinnerthaler M, Bischof J, Streubel MK, et al. Oxidative Stress in Aging Human Skin.
524 Biomolecules 2015;5:545–589.
- 525 [12] Wagener FADTG, Carels CE, Lundvig DMS. Targeting the Redox Balance in
526 Inflammatory Skin Conditions. Int J Mol Sci 2013;14:9126–9167.
- 527 [13] Carotenuto R, Fogliano C, Rienzi M, et al. Comparative Toxicological Evaluation of
528 Tattoo Inks on Two Model Organisms. Biology (Basel) 2021;10:1308.
- 529 [14] Høgsberg T, Jacobsen NR, Clausen PA, et al. Black tattoo inks induce reactive oxygen
530 species production correlating with aggregation of pigment nanoparticles and product
531 brand but not with the polycyclic aromatic hydrocarbon content. Exp Dermatol
532 2013;22:464–469.
- 533 [15] Neale PA, Stalter D, Tang JYM, et al. Bioanalytical evidence that chemicals in tattoo
534 ink can induce adaptive stress responses. J Hazard Mater 2015;296:192–200.
- 535 [16] Amaral GP, Puntel GO, Dalla Corte CL, et al. The antioxidant properties of different
536 phthalocyanines. Toxicol In Vitro 2012;26:125–132.
- 537 [17] Qing F, Li L, Yongyan H, et al. Studies on metal phthalocyanine as a dual functional
538 mimic enzyme. Journal of Tongji Medical University 2001;21:13–16.
- 539 [18] Hadwan MH. Simple spectrophotometric assay for measuring catalase activity in
540 biological tissues. BMC Biochemistry 2018;19:7.
- 541 [19] Homolak J, Babic Perhoc A, Knezovic A, et al. The Effect of Acute Oral Galactose
542 Administration on the Redox System of the Rat Small Intestine. Antioxidants
543 2022;11:37.
- 544 [20] Homolak J, Perhoc AB, Joja M, et al. Non-alcoholic components of Pelinkovac, a
545 Croatian wormwood-based strong liquor, counteract the inhibitory effect of high ethanol
546 concentration on catalase in vitro. BioRxiv 2022;2022.01.07.475357.
- 547 [21] Li X. Improved Pyrogallol Autoxidation Method: A Reliable and Cheap Superoxide-
548 Scavenging Assay Suitable for All Antioxidants. J Agric Food Chem 2012;60:6418–
549 6424.
- 550 [22] Marklund S, Marklund G. Involvement of the superoxide anion radical in the
551 autoxidation of pyrogallol and a convenient assay for superoxide dismutase. Eur J
552 Biochem 1974;47:469–474.
- 553 [23] Graham ML, Prescott MJ. The multifactorial role of the 3Rs in shifting the harm-benefit
554 analysis in animal models of disease. Eur J Pharmacol 2015;759:19–29.
- 555 [24] Parekh BS, Mehta HB, West MD, et al. Preparative elution of proteins from
556 nitrocellulose membranes after separation by sodium dodecyl sulfate-polyacrylamide
557 gel electrophoresis. Anal Biochem 1985;148:87–92.
- 558 [25] Caplins BW, Mullenbach TK, Holmes RJ, et al. Femtosecond to nanosecond excited
559 state dynamics of vapor deposited copper phthalocyanine thin films. Phys Chem Chem
560 Phys 2016;18:11454–11459.

561 [26] Farag AAM. Optical absorption studies of copper phthalocyanine thin films. *Optics &*
562 *Laser Technology* 2007;39:728–732.

563 [27] Hirakawa K. *Fundamentals of Medicinal Application of Titanium Dioxide*
564 *Nanoparticles*. IntechOpen; 2015.

565 [28] Monteiller C, Tran L, MacNee W, et al. The pro-inflammatory effects of low-toxicity
566 low-solubility particles, nanoparticles and fine particles, on epithelial cells in vitro: the
567 role of surface area. *Occup Environ Med* 2007;64:609–615.

568 [29] Schwotzer D, Niehof M, Schaudien D, et al. Cerium oxide and barium sulfate
569 nanoparticle inhalation affects gene expression in alveolar epithelial cells type II. *J*
570 *Nanobiotechnology* 2018;16:16.

571 [30] Delaval M, Wohlleben W, Landsiedel R, et al. Assessment of the oxidative potential of
572 nanoparticles by the cytochrome c assay: assay improvement and development of a
573 high-throughput method to predict the toxicity of nanoparticles. *Arch Toxicol*
574 2017;91:163–177.

575 [31] Li M, Yin J-J, Wamer WG, et al. Mechanistic characterization of titanium dioxide
576 nanoparticle-induced toxicity using electron spin resonance. *Journal of Food and Drug*
577 *Analysis* 2014;22:76–85.

578 [32] Zhang H-M, Cao J, Tang B-P, et al. Effect of TiO₂ nanoparticles on the structure and
579 activity of catalase. *Chemico-Biological Interactions* 2014;219:168–174.

580 [33] Song U, Jun H, Waldman B, et al. Functional analyses of nanoparticle toxicity: a
581 comparative study of the effects of TiO₂ and Ag on tomatoes (*Lycopersicon*
582 *esculentum*). *Ecotoxicol Environ Saf* 2013;93:60–67.

583 [34] Bocca B, Sabbioni E, Mičetić I, et al. Size and metal composition characterization of
584 nano- and microparticles in tattoo inks by a combination of analytical techniques. *J Anal*
585 *At Spectrom* 2017;32:616–628.

586 [35] Høgsberg T, Loeschner K, Löf D, et al. Tattoo inks in general usage contain
587 nanoparticles. *Br J Dermatol* 2011;165:1210–1218.

588 [36] Manke A, Wang L, Rojanasakul Y. Mechanisms of nanoparticle-induced oxidative
589 stress and toxicity. *Biomed Res Int* 2013;2013:942916.

590

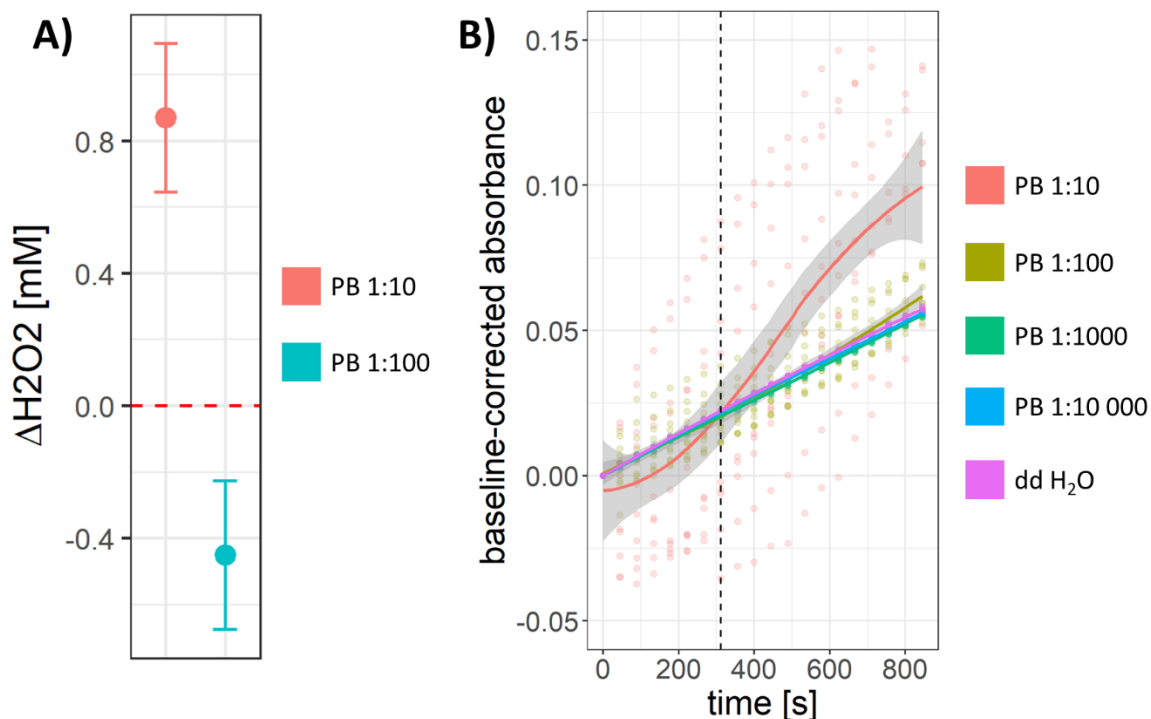


Fig 1. Catalase (CAT) and superoxide dismutase (SOD)-like activity of Persian Blue tattoo ink (PB) *in vitro*. A) Output of the model including the tested dilutions and substrate concentrations demonstrating dilution-dependent CAT-like activity of PB, with the 1:10 PB dilution acting as CAT mimetic (substrate concentrations: 6, 8, and 10 mM H₂O₂; t = 300 s). B) Dilution-dependent SOD-like activity of PB, with 1:10 PB demonstrating SOD-like properties at t < 300 s, and potentiation of 1,2,3-trihydroxybenzene autooxidation at t > 300 s. 1:100, 1:1000 and 1:10 000 dilutions show no SOD-mimetic activity.

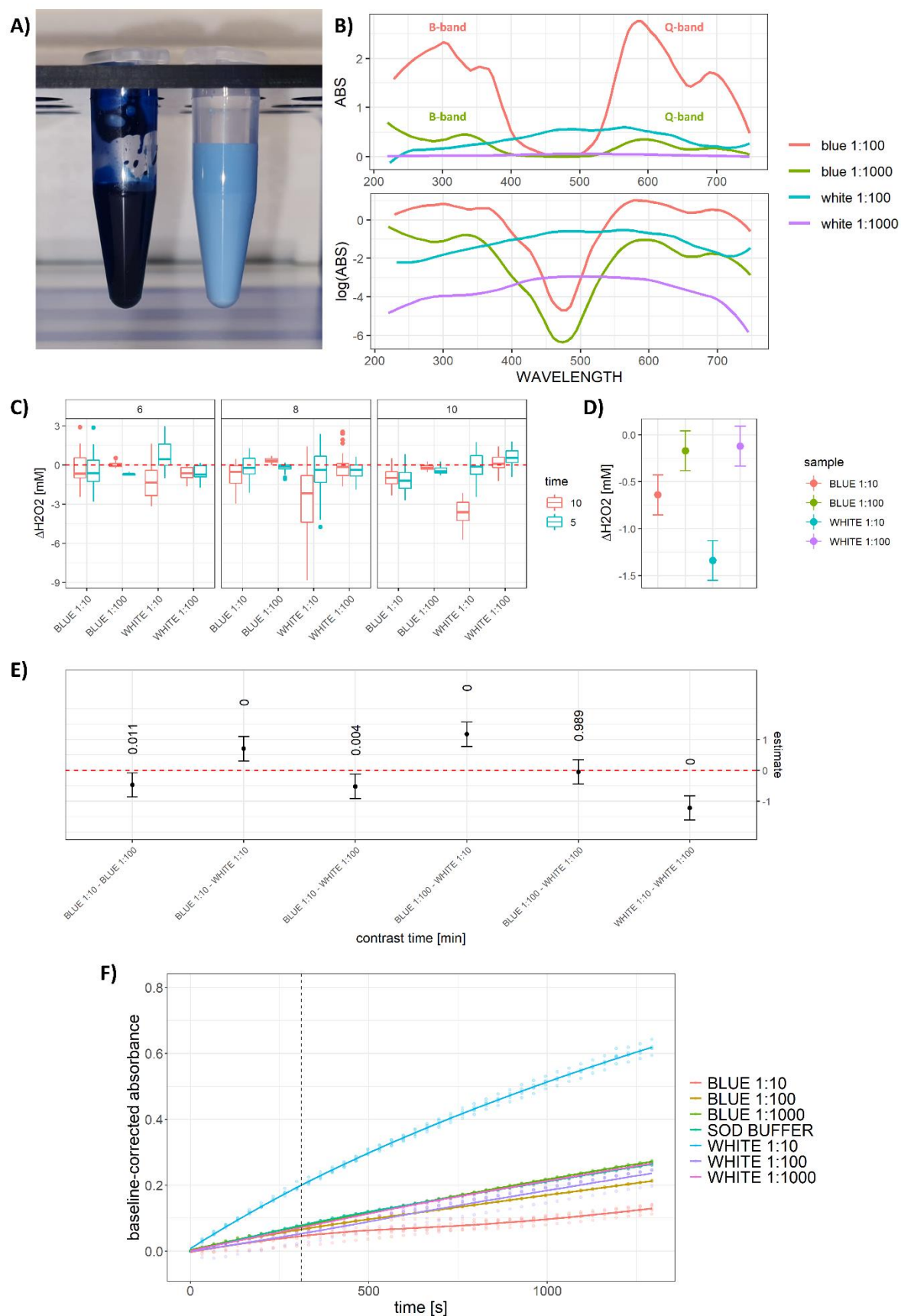


Fig 2. Catalase (CAT) and superoxide dismutase (SOD)-like activity of blue and white fractions of the Persian Blue tattoo ink (PB) *in vitro*. A) A representative image of the blue

(left) and white (right) fractions of PB. B) Absorption spectra of the 1:100 (red) and 1:1000 (green) dilution of the blue fraction, and the 1:100 (turquoise) and 1:1000 (purple) dilution of the white fraction of PB. The absorption spectrum of the blue fractions demonstrates the Soret peak (B-band) and Q-band, strongly indicating that copper phthalocyanine was only present in the blue fraction of PB. C) Results demonstrating no CAT-like activity of different dilutions of either fraction *in vitro* (substrate concentrations: 6, 8, 10 mM H₂O₂; t₁= 300 s; t₂= 600 s). D) Output of the model including tested dilutions of the blue and white fraction, time, and substrate concentration, demonstrating no observed CAT-like activity. E) Comparison of the observed CAT-like activities of two dilutions of the blue and white fraction at different substrate concentrations. P-values are reported above estimates of differences of estimated marginal means accompanied by 95% confidence intervals. F) Dilution-dependent SOD-like activity of PB fractions. The 1:10 dilution of the white fraction potentiates autooxidation of 1,2,3-trihydroxybenzene at t < 300 s, while all other dilutions of both fractions show no pronounced effects. At t > 300 s, the 1:10 dilution of the blue fraction demonstrates pronounced, while the 1:100 dilution shows slightly less pronounced SOD-like activity. The 1:10 dilution of the white fraction shows a strong 1,2,3-trihydroxybenzene autooxidation potentiating effect.

619

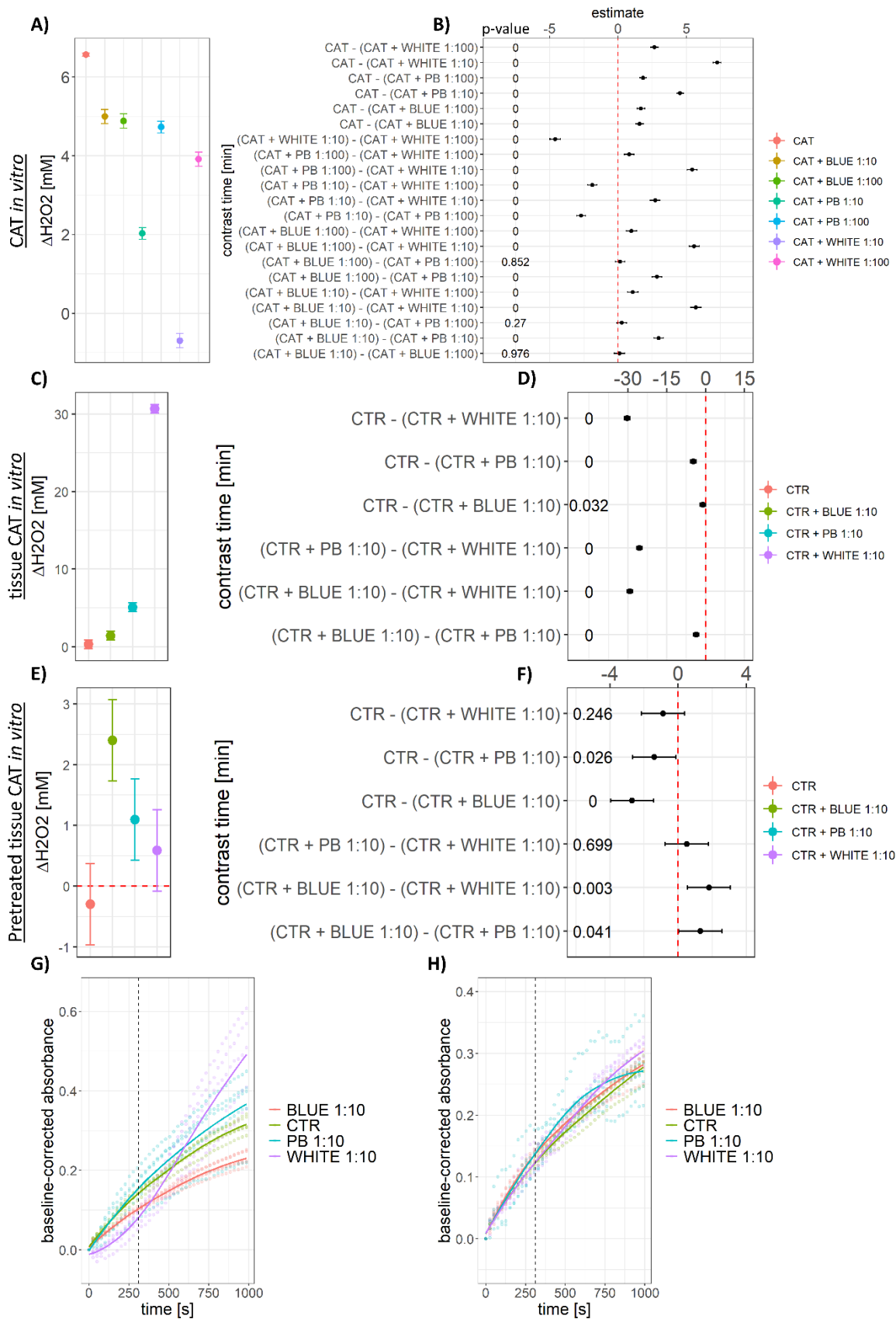


Fig 3. Catalase (CAT) and superoxide dismutase (SOD)-like activity of the Persian Blue tattoo ink (PB) and its blue and white fractions *in vitro* in the presence of biochemical constituents of the skin. A) Output of the model including tested dilutions of PB and its blue and white

fractions and substrate concentrations (6, 8, and 10 mM H₂O₂), demonstrating the ability of PB and its fractions to inhibit CAT *in vitro* (t = 60 s). While the effect was not dose-dependent for the blue fraction, the white fraction and PB showed a pronounced dose-dependent inhibition of the enzyme. B) Model results presented as point estimates of differences of estimated marginal means with 95 % confidence intervals for the model presented in A. C) Output of the model including tested dilutions of PB and the blue and white PB fractions demonstrating the ability of the samples to potentiate CAT activity in the complex biochemical matrix of normal skin tissue (substrate concentration: 10 mM H₂O₂; t = 600 s). D) Model results presented as point estimates of differences of estimated marginal means with 95 % confidence intervals for the model presented in C. E) Output of the model including tested dilutions of PB and the blue and white PB fractions demonstrating the effect of the samples on CAT activity in the complex biochemical matrix of normal skin tissue following pre-incubation of the dyes with the tissue samples (pre-incubation time: 180 min; pre-incubation temperature: 37 °C; substrate concentration: 10 mM H₂O₂; t = 600 s). F) Model results presented as point estimates of differences of estimated marginal means with 95 % confidence intervals for the model presented in E. G) SOD mimetic activity of PB and the blue and white PB fractions in the complex biochemical matrix of normal skin tissue. At t < 300 s, PB demonstrated no SOD-like activity, while both blue and white fractions acted as SOD mimetics. At t > 300 s, PB was associated with slight potentiation, while the white PB fraction induced pronounced autooxidation of 1,2,3-trihydroxybenzene. Conversely, the blue PB fraction demonstrated SOD-mimetic activity. H) SOD mimetic activity of PB and the blue and white PB fractions in the complex biochemical matrix of normal skin tissue following incubation of the dyes with skin tissue for 180 min at 37 °C. Pre-incubation of the dyes with the skin tissue constituents alleviated the effects observed in F.

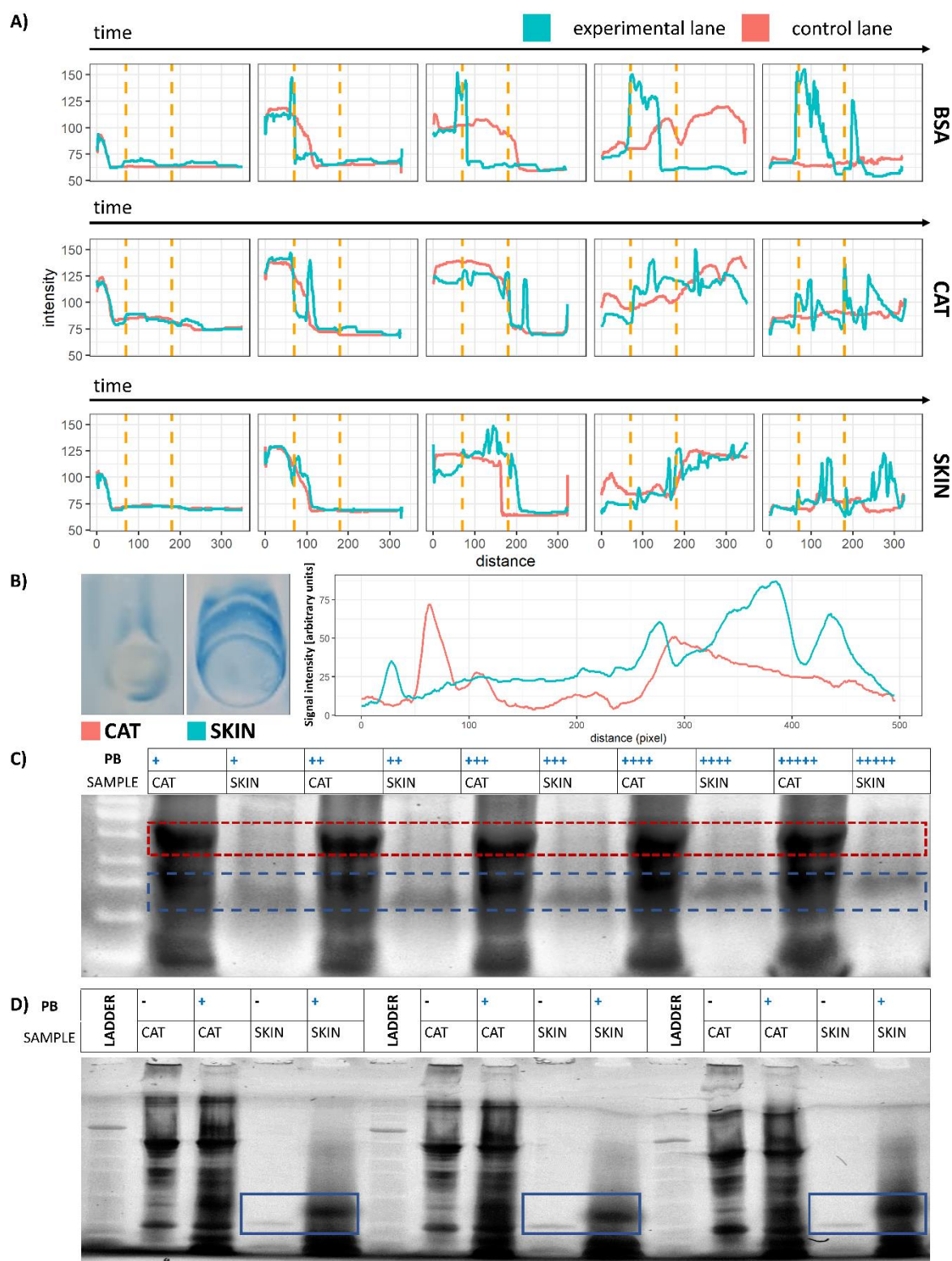
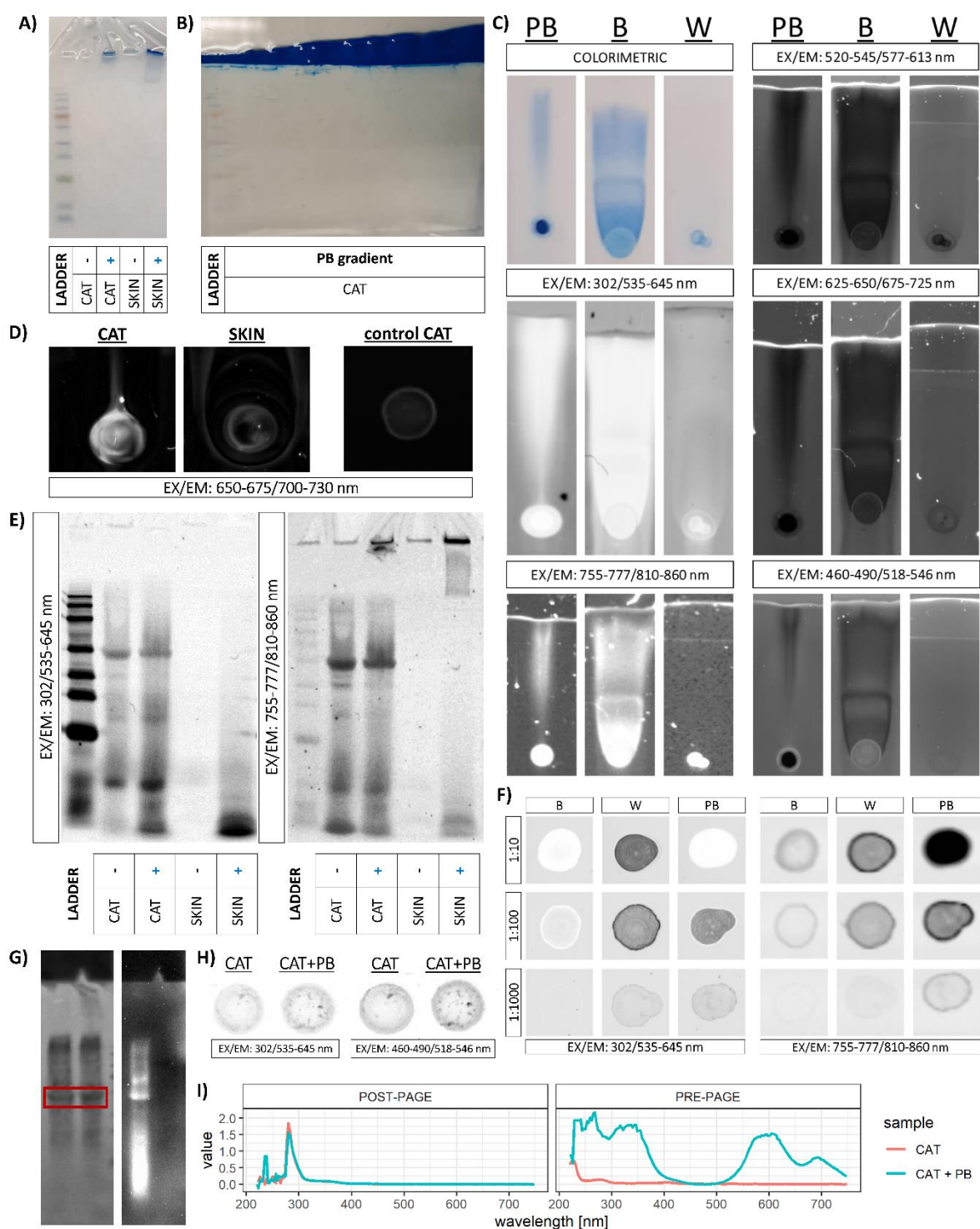


Fig 4. Interaction of the blue tattoo ink with constituents of the skin homogenate assessed by the lateral flow assay (LFA), CuPC-capturing gradient electrophoretic mobility shift assay (CCG-EMSA), and sample pre-incubation electrophoretic mobility shift assay (SP-EMSA). A) Line profiles obtained from LFA with the Persian Blue (PB) tattoo ink used as a mobile phase. Profiles obtained from the free route for the uninterrupted analyte flow (control lane) and the sample-capturing lane containing two capturing pools (experimental lane; capturing pools are marked with yellow lines) are shown for the control high binding capacity protein – bovine

serum albumin (BSA; top), catalase (CAT; middle), and the skin homogenate (SKIN; bottom). Both time (5 time-points) and the direction of the flow are aligned with the X-axis. B) CAT and skin homogenate after LFA with PB mobile phase followed by ddH₂O (left). The skin sample shows a wave pattern suggesting the presence of interaction with several separate components. Line profiles of the samples presented on the left with 3 peaks associated with the skin sample suggest heterogeneous interaction patterns. C) The polyacrylamide gel from the CCG-EMSA experiment demonstrates the absence of the electrophoretic mobility shift for the CAT sample (red), and dose-dependent electrophoretic deceleration for the skin sample (blue). The trichalo-containing polyacrylamide gel was visualized using 302 nm excitation and 535-645 nm emission. A negative image is presented. D) The gel from the SP-EMSA experiment showing 3 technical replicates of pre-treated and untreated CAT and skin samples with no apparent deceleration in the CAT sample, and a prominent reduction in mobility of the prominent peak in the skin sample (blue). The trichalo-containing polyacrylamide gel was visualized using 302 nm excitation and 535-645 nm emission. A negative image is presented.

670



671

672 **Fig 5.** Interaction of the blue tattoo ink with constituents of the skin homogenate assessed by
 673 the lateral flow assay (LFA), CuPC-capturing gradient electrophoretic mobility shift assay
 674 (CCG-EMSA), and sample pre-incubation electrophoretic mobility shift assay (SP-EMSA)
 675 spectral analysis. A) Native image of the polyacrylamide gel from the SP-EMSA experiment
 676 after electrophoretic separation of catalase (CAT) and skin samples. B) Native image of the
 677 polyacrylamide gel from the CCG-EMSA experiment after electrophoretic separation. C)
 678 Spectral analysis of the LFA membranes using different excitation and emission wavelengths

demonstrates 3 general patterns: the sample pool (the area where the sample was deposited – lower portion of the images); the middle mobile phase (largely absent in the white fraction – the middle portion of the images); and the mobile front (present in all samples – upper portion of the images). D) CAT and the skin sample exposed to the Persian Blue tattoo ink (PB) mobile phase, and the control CAT sample (not exposed to the PB mobile phase to control for baseline spectral properties) emission at 700-730 nm upon excitation at 650-675 nm. A substantial increment in emission and the smearing pattern speak in favor of the interaction of CAT with the PB mobile front. E) Spectral analysis of the gel from the SP-EMSA experiment shows that both the PB-pretreated skin sample and PB-pretreated CAT emit a signal in concordance with the presence of constituents from the white fraction (see F). Notice the difference in the signal from the stacking gel and the resolving gel in the context of the ink fractions emission signals (presented in F). Negative images are presented. F) The effect of PB fractions and concentrations in two different spectral planes. Negative images are presented. G) Ponceau S staining of the nitrocellulose membrane with the PB-treated and PB-untreated CAT from the SP-EMSA experiment (left), and the corresponding membrane exposed to luminol and H₂O₂ demonstrating a substantial H₂O₂ dissociation potential only in the PB-treated CAT sample (right). The main CAT fraction is emphasized in red. The pattern indicates that both the PB-pretreated CAT and the front have the ability to promote H₂O₂ dissociation. H) Negative images of the signal obtained from the PB-treated and PB-untreated CAT eluted from the membrane shown in G in two different spectral planes indicating the presence of the constituents associated with the white fraction. I) Confirmation of the absence of the CuPC from the samples containing CAT eluted from the membrane shown in G. UV-Vis spectra both CAT and PB-pretreated CAT before the polyacrylamide gel electrophoresis (PRE-PAGE) and after elution from the membrane (POST-PAGE).